



# Characterizing thermal and mechanical properties of graphene/epoxy nanocomposites



Sung-Chiu Shiu, Jia-Lin Tsai\*

Department of Mechanical Engineering, National Chiao Tung University, Hsinchu 300, Taiwan, ROC

## ARTICLE INFO

### Article history:

Received 6 September 2012

Received in revised form 4 September 2013

Accepted 7 September 2013

Available online 17 September 2013

### Keywords:

A. Nano-structures

B. Mechanical properties

B. Thermal properties

Molecular dynamics simulation

## ABSTRACT

This study aims to investigate the thermal and mechanical properties of graphene/epoxy nanocomposites using molecular dynamics (MD) simulation. Three different formats of graphene: graphene flakes, intercalated graphene and intercalated graphene oxide, were incorporated respectively in an epoxy matrix to form the graphene/epoxy nanocomposites. The mechanical properties of the graphene/epoxy nanocomposites, including Young's modulus ( $E$ ), glass transition temperature ( $T_g$ ) and coefficient of thermal expansion (CTE), in terms of three different formats of graphene, were characterized in this study. In addition to the mechanical properties, the influences of graphene on the density distribution of epoxy polymers in the nanocomposites were also examined. The results showed that the local density in the vicinity of the graphene is relatively high, and then progressively decreases to the bulk value in regions further away from the interface. On the other hand, for the mechanical and thermal properties, the nanocomposites with intercalated graphene exhibit a higher Young's modulus, a higher glass transition temperature and a lower thermal expansion coefficient than do those with graphene flakes. This is because the intercalated graphene can lead to a high amount of high density polymer in the nanocomposites, and thus enhance the overall properties of the nanocomposites. In addition, the intercalated graphene oxide provides the best reinforcement of the three systems of nanocomposites. Based on the calculation of interaction energy, it appears that the oxide modification of the graphene surface can effectively lead to the high interaction energy, such that the graphene oxide can demonstrate a relatively high reinforcing efficiency.

© 2013 Elsevier Ltd. All rights reserved.

## 1. Introduction

Graphene is a monolayer structure in which the carbon atoms are arranged in a hexagonal pattern. The interatomic distance between the adjacent carbon atoms is 1.42 Å, and the associated atomistic interaction is covalently bonded by  $sp^2$  hybridized electrons. With the employment of micromechanical cleavage, Novoselov et al. [1] successfully isolated the individual graphene from graphite bulk materials. Experiments indicated that the graphene exhibits a high modulus of 1 TPa and a high strength of 130 GPa [2]. In addition to the superior mechanical properties, the high specific surface of the 2D layer structure makes the graphene a potential reinforcement in nanocomposites. Several researches have incorporated graphene sheets into epoxy resin to form the nanocomposites, indicating that the modulus and glass transition temperature of the nanocomposites can be effectively increased [3–8]. In addition, a decreasing tendency of the coefficients of thermal expansion associated with the improved thermal stability was also observed in the epoxy-based nanocomposites reinforced with

graphene sheets [4,5]. Shen et al. [3] introduced graphene sheets into epoxy resin and investigated the mechanical properties of the nanocomposites at room temperature and at a cryogenic temperature of 77 K, respectively. It was discovered that with 0.5 wt% of graphene sheets, the modulus of the epoxy was increased from 2 GPa to 3.1 GPa at room temperature, and from 5.9 GPa to 7.4 GPa at cryogenic temperature. An increasing tendency in modulus was also noted by Lee et al. [4], who examined the mechanical and thermal properties of epoxy in conjunction with graphene sheets at various temperatures. They showed that the glass transition temperature of graphene nanocomposites was raised, and the corresponding coefficient of thermal expansion was reduced. Wang et al. [5] investigated the thermal properties of graphene nanocomposites, revealing that graphene can effectively improve the thermal stability of epoxy polymer. A higher glass transition temperature in epoxy nanocomposites caused by the addition of graphene sheet was also observed by Martin-Gallego et al. [6,7], who fabricated and tested UV cured nanocomposites. Tang et al. [8] explored the effect of graphene dispersion on the mechanical properties of graphene/epoxy nanocomposites. It was shown that the nanocomposites with highly dispersed graphene exhibit higher strength and fracture toughness than those with poorly dispersed graphene.

\* Corresponding author. Tel.: +886 3 5731608; fax: +886 3 5720634.

E-mail address: [jjalin@mail.nctu.edu.tw](mailto:jjalin@mail.nctu.edu.tw) (J.-L. Tsai).

Rafiee et al. [9] compared the mechanical performances of epoxy resin reinforced by graphene platelets, single walled carbon nanotubes and multiwall carbon nanotubes. It was shown that in terms of the same amount of reinforcement, the nanocomposites in conjunction with graphene platelets exhibit higher modulus and strength than the other two nanocomposites.

In addition to the epoxy polymer, the improved thermal and mechanical properties in other polymer systems have also been reported [10–21], and it appears that the graphene sheet can efficiently modify the mechanical performances and thermal stability of the polymeric nanocomposites. However, the influence of the dispersion of the graphene sheet, as well as the morphology of the epoxy resin on the behavior of the nanocomposites has rarely been explored in the available literature. Furthermore, the effect of the functional groups adhered onto the graphene associated with the mechanical properties of nanocomposites has also seldom been investigated. In this study, three different formats of graphene sheets: intercalated graphene, intercalated graphene oxide and graphene flakes, were incorporated respectively in an epoxy matrix to form graphene nanocomposites. The mechanical properties of the nanocomposites, including Young's modulus, glass transition temperature and thermal expansion coefficient, in terms of different formats of graphene, were characterized. Moreover, the influences of graphene on the morphology and density of nearby polymers were examined, and the underlying mechanism resulting in the improvement of the mechanical properties of nanocomposites was discussed. The influence of surface modification, in terms of the interfacial bonding energy on the mechanical properties of graphene nanocomposites, was also investigated.

## 2. Graphene/epoxy nanocomposites

In order to explore the mechanical properties and morphologies of graphene/epoxy nanocomposites using MD simulation, atomistic models of nanocomposites were first constructed. Three different formats of graphene: intercalated graphene, intercalated graphene oxide and graphene flakes, were incorporated, respectively, in epoxy matrix to form the graphene nanocomposites. For the nanocomposites with graphene flakes, the molecular model consists of an eight-layer graphite (stacked along the *z* direction in A-B sequence) and 96 epoxy units exposed randomly on each side of the graphite. It must be noted that the epoxy is a cross-linked polymer, and the consideration of the cross-linking behavior in MD simulation based on probability is too time consuming to be applied to a larger model. In order to save on computing cost, a representative cross-linked unit proposed by Yu et al. [22] was employed to denote the cross-linked epoxy where three molecular chains of EPON862<sup>®</sup> resin were incorporated with one molecular chain of TETA<sup>®</sup> curing agent, as shown in Fig. 1. On the other hand, for the nanocomposites with intercalated graphene, three graphene sheets deployed homogeneously within the molecular model, in which 36 epoxy units were intercalated randomly between the graphene sheets. In addition to the intercalated graphene, the graphene modified with the hydroxyl group and epoxy group which were commonly observed in the experiments [23] was also considered in the atomistic model. The graphene with surface modification is shown in Fig. 2(a). Basically, the ratio of hydroxyl group (shown in Fig. 2(b)) to epoxy group (shown in Fig. 2(c)) is assumed to be 1:1.5 [24], and the modification ratio [25], defined as the number of surfactant atoms divided by the atom number of graphene, is 10%. Note that in the above atomistic model, the graphene with dimensions of 26.47 Å and 26.81 Å is embedded in the epoxy polymer, and the weight fraction of the graphene with respect to the nanocomposites considered in this study is around

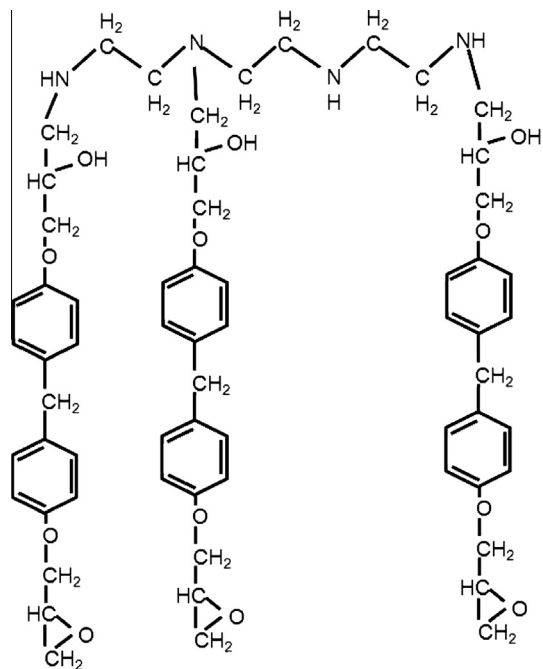


Fig. 1. Representative unit of epoxy polymer [22].

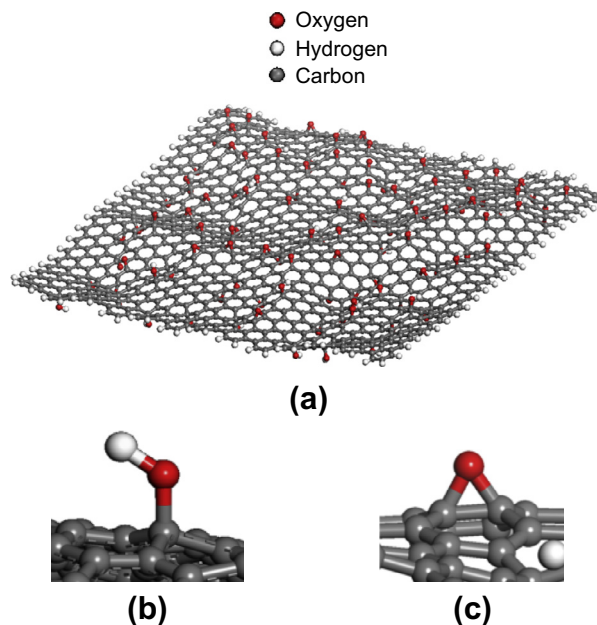


Fig. 2. (a) Atomistic structures of graphene oxide, (b) hydroxyl group and (c) epoxy group.

18%. In the MD simulations, the atomistic interactions between the atoms are described using a potential function. In general, there are two kinds of potential functions considered in the atomistic system: one is the bonded potential, such as the covalent bond, and the other is the non-bonded potential, such as the van der Waals force. For the graphene/epoxy nanocomposites, the covalent bonding, as well as the non-bonding interaction among the molecular chains was described by the COMPASS force field [26].

The equilibrated molecular structure of epoxy/graphene nanocomposites with minimized energy was accomplished by sequentially performing the NVT and NPT ensembles in the MD

simulation, with a time increment of 1 fs. The NVT ensemble was conducted at 1100 K for 200 ps, the purpose of which was to supply enough kinetic energy to the epoxy molecules so that homogeneous molecular structure within the simulation box could be achieved. After this, the temperature was designated to 600 K for another 200 ps in the NVT ensemble. In the NVT ensemble, the carbon atoms on the graphene were fixed at their original position throughout the simulation. Subsequently, the NPT ensemble was performed at 0 atm in order to achieve a stress-free state, and at the same time the corresponding temperature was gradually reduced from 600 K to 1 K. In fact, there were two sub-steps introduced during the cooling process. In the first sub-step, the temperature was designated at 300 K, and the simulation time was 200 ps. In the beginning of the first sub-step, the frozen atoms of graphite were released so that the entire nanocomposites system could be equilibrated under a stress-free condition. In the second sub-step, the target temperature was 1 K, and the simulation time was also set to 200 ps. During the simulation, the total potential energy variation was examined, and when the quantity fluctuated around a certain mean value for a while, the system was considered to be in a state of energy minimization. Note that NVT ensemble stands for the number of atoms ( $N$ ), volume ( $V$ ) and temperature ( $T$ ) being fixed during the simulation, and NPT ensemble indicates that the number of atoms ( $N$ ), pressure ( $P$ ) and temperature ( $T$ ) remain constant during the simulation. The MD simulations for graphite/epoxy nanocomposites were carried out using a commercial code, Materials Studio, developed by Accelrys Inc. [27]. The dimensions of the simulation cell under energy minimization condition for the stacked and intercalated graphene nanocomposites are shown in Fig. 3. Subsequently, the morphology, as well as the mechanical properties of the nanocomposites was then characterized from the simulation cell of the nanocomposites.

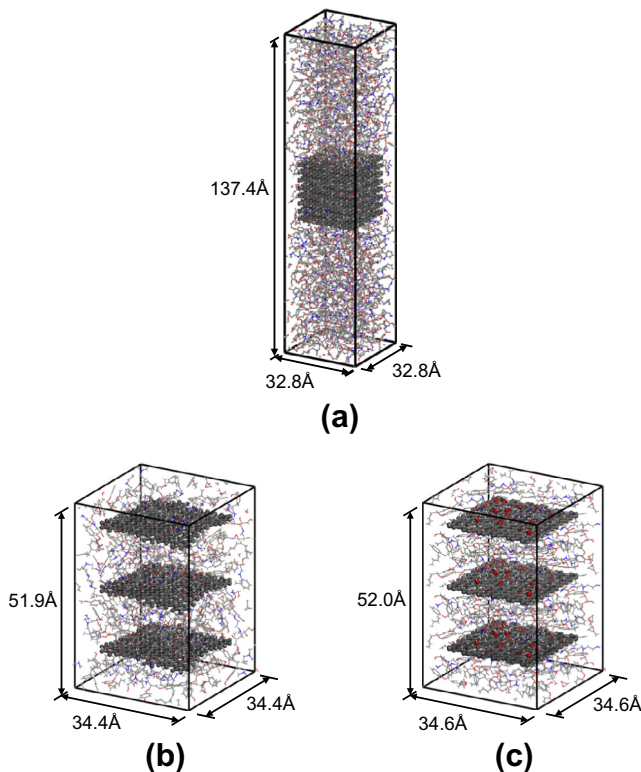


Fig. 3. Atomistic structures of epoxy nanocomposites ((a) graphene flakes, (b) intercalated graphene and (c) intercalated graphene oxide).

### 3. Observation of molecular configuration

The influence of graphite on the molecular configuration of epoxy was investigated by observing the density variations of epoxy molecular chains. This can be done by partitioning the epoxy along the  $z$  axis into several small regions, as shown in Fig. 4. It must be noted that the position  $z = 0$  denotes the central section of the simulation cell, and the partition size  $\Delta z = z_{i+1} - z_i$  indicating the thickness of each small region is around 1 Å. In each small region, the total atomic mass and the corresponding volume were calculated, and then the density was calculated as the mass divided by the associated volume. The density distributions of epoxy polymer with the nanocomposites along the  $z$  axis are shown in Fig. 5. It can be seen that for the nanocomposites with graphene flakes, the density near the graphite/epoxy interface is higher, and then rapidly decreases to the bulk value of 1.23 g/cc [28] (indicated by the horizontal dash line), as the location is a small distance from the interface. In addition, the density distributions of epoxy in the nanocomposites with intercalated graphene are shown in Fig. 5, where the vertical dash lines denote the interface between the intercalated graphene and the epoxy. It appears that on both sides of the graphene, the polymer density is relatively high. As compared to the graphene flakes, the dispersed graphene may lead to a greater amount of epoxy with high density because more interfacial areas were generated in the intercalated nanocomposites. Moreover, the increased amount of high density polymer may have more appreciable influence in the mechanical properties of nanocomposites, which will be discussed in the next section.

### 4. Determination of thermal and mechanical properties of graphene/epoxy nanocomposites

#### 4.1. Young's modulus

In addition to the density distribution of epoxy polymer, the mechanical properties of the molecular structures of nanocomposites were characterized using MD simulation. By applying a small amount of strain component to the simulation cell in one direction, while the other strain components remained fixed, the deformed state of the simulation cell, as shown in Fig. 6, was generated. After conducting the NVT ensemble for 400 ps, the energy minimization condition of the deformed state was attained, and the stress components of the simulation cell associated with the deformed configuration were then calculated using the virial theorem [29]:

$$\sigma = -\frac{1}{V_0} \left( \sum_{i < j} r_{ij} f_{ij} \right) \quad (1)$$

where  $r_{ij}$  and  $f_{ij}$  denote the atomic distance and the corresponding interaction force between any two atoms, respectively.  $V_0$  represents the total volume of the simulation cell. In Eq. (1), because the model was simulated at 1 K, the temperature effect was neglected in the stress computation. By following the concept of continuum mechanics, the constitutive relation of nanocomposites in terms of the stiffness matrix  $[C]$  can be calculated as the derivative of the stress associated with the corresponding strain component. The explicit form for the normal stress and normal strain relation can be expressed as:

$$\begin{bmatrix} \sigma_{xx} \\ \sigma_{yy} \\ \sigma_{zz} \end{bmatrix} = \begin{bmatrix} C_{xx} & C_{xy} & C_{xz} \\ C_{yx} & C_{yy} & C_{yz} \\ C_{zx} & C_{zy} & C_{zz} \end{bmatrix} \begin{bmatrix} \varepsilon_{xx} \\ \varepsilon_{yy} \\ \varepsilon_{zz} \end{bmatrix}$$

where  $[C]$  is the stiffness matrix. In this study, the small amounts of extension were employed respectively in the  $x$ ,  $y$  and  $z$  directions, and the corresponding stress components were calculated from

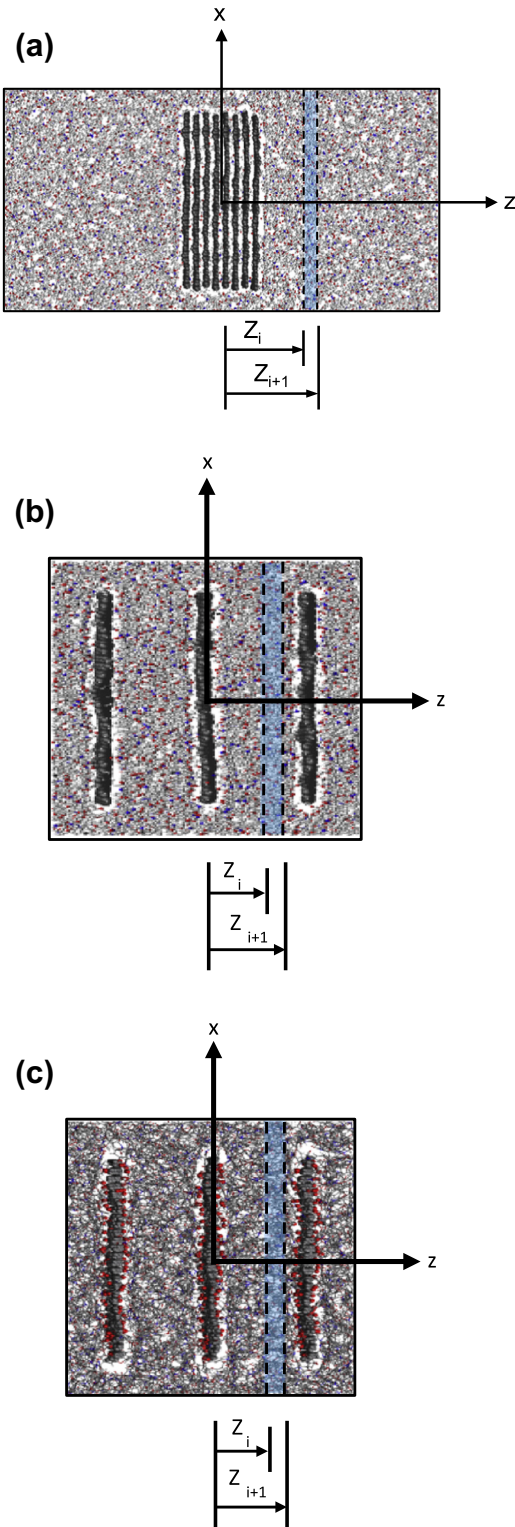


**Fig. 4.** Partitioning the epoxy from  $z = z_0$  along  $z$  axis into several small regions in nanocomposites ((a) graphene flakes, (b) intercalated graphene and (c) intercalated graphene oxide).

Eq. (1). By taking the inverse of the stiffness matrix, the compliance matrix  $[S]$ , in terms of engineering constants, is derived as:

$$[S] = [C^{-1}] = \begin{bmatrix} \frac{1}{E_x} & \frac{-\nu_{yx}}{E_y} & \frac{-\nu_{zx}}{E_z} \\ \frac{-\nu_{xy}}{E_x} & \frac{1}{E_y} & \frac{-\nu_{yz}}{E_z} \\ \frac{-\nu_{xz}}{E_x} & \frac{-\nu_{yz}}{E_y} & \frac{1}{E_z} \end{bmatrix} \quad (3)$$

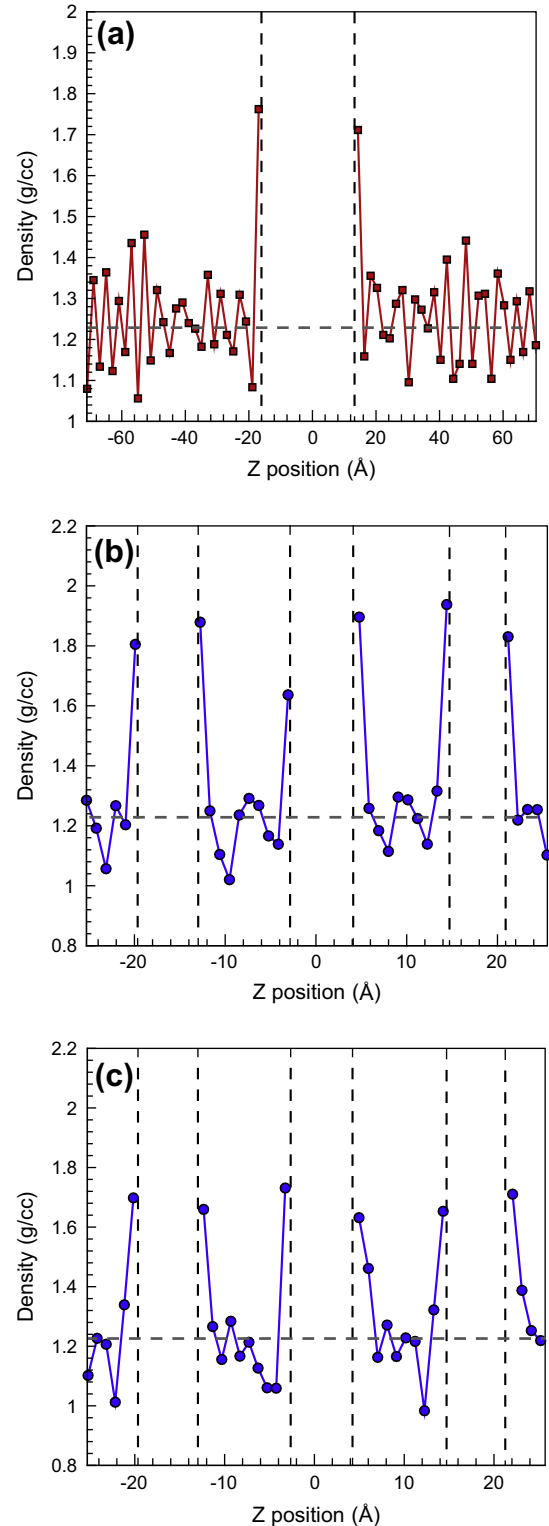


**Fig. 5.** Density distribution of epoxy in graphene nanocomposites ((a) graphene flakes, (b) intercalated graphene and (c) intercalated graphene oxide).

from which the elastic properties of the materials were obtained. In Eq. (3),  $E$  denotes Young's modulus, and  $\nu$  designates Poisson's ratio. With the microstructures of the simulation cell shown in Fig. 3, the nanocomposites were assumed to be orthotropic and, in theory, the mechanical properties in the  $x$  and  $y$  directions should coincide. However, because there is variation in the atomistic simulation, the properties in the two directions may not be the same. Thus,

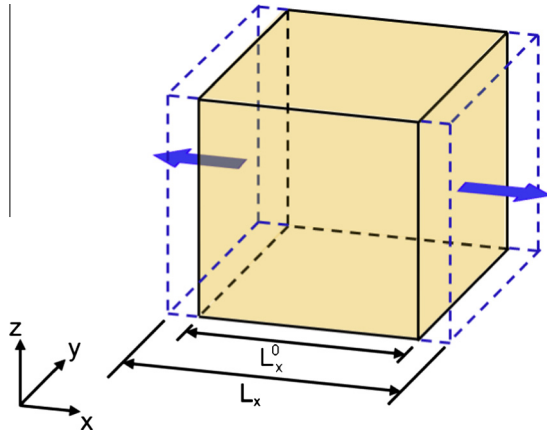


Fig. 6. Extension of simulation cell in one direction.

the averaged value of  $E_x$  and  $E_y$  was regarded as the in-plane modulus of the nanocomposites. The moduli of the nanocomposites in terms of the three different formats of graphene are listed in Table 1. For comparison, the modulus of pristine epoxy is also included in the same table. Basically, the epoxy was assumed to be isotropic, and thus the properties obtained in  $x$ ,  $y$  and  $z$  directions were taken in average, and then presented in the table. It can be seen that the addition of the graphene can effectively improve the moduli of the epoxy, and the extent of the increase is dependent on the formats of the graphene. The intercalated graphene is generally superior to the graphene flakes, and the intercalated graphene oxide provides the best reinforcement among the cases. In fact, from the density distribution of the epoxy, it can be seen that more interfaces are generated by the intercalated graphene, and a greater amount of high density polymer is created in the intercalated nanocomposites. Thus, the moduli of the intercalated nanocomposites are higher than those of the nanocomposites with graphene flakes. The degree of dispersion resulting in the change of morphology of epoxy is an essential factor influencing the properties of nanocomposites. In addition to the dispersion, the oxide functional group on the graphene is the other important factor which may influence the mechanical properties of the graphene nanocomposites. The effect of surface modification will be elaborated from the computation of the interaction energy between the graphene and surrounding epoxy polymers in the next section.

#### 4.2. Glass transition temperature

Glass transition temperature ( $T_g$ ) is a physical property at which a material changes from a glassy state to a rubbery state. The effect of the graphene on the  $T_g$  of nanocomposites was explored in MD simulation, in which the temperature was varied from 600 K to 200 K step by step with a temperature difference of 20 K. In each step, the NPT ensemble was adopted for 100 ps, so that the configuration with energy minimization could be accomplished. When the volume of the simulation cell was determined from MD simulation, the corresponding density was then

computed. The density variation of the nanocomposites associated with temperature variation is shown in Fig. 7. By taking the bi-linear curve-fitting of the data, the intersection of the two linear curves was recognized as the  $T_g$  of the sample. From Fig. 7(a), it seems that the  $T_g$  value of pristine epoxy is 380 K, which is quite compatible with the experimental data of 377 K [30]. For the nanocomposites, the density variations associated with the temperature change are shown in Fig. 7(b)–(d). The corresponding values of the  $T_g$  for the nanocomposites are summarized in Table 1. It can be seen that  $T_g$  increases as the graphene is incorporated in the nanocomposites, and the intercalated nanocomposites exhibit higher  $T_g$  than do the nanocomposites with graphene flakes. It is interesting to note that the oxide modification of graphene has no significant influence on the value of  $T_g$ . The reason for this could be that  $T_g$  is sensitive to the morphology of the epoxy polymer in the vicinity of graphene, but not to the surface modification of graphene.

#### 4.3. Coefficient of thermal expansion

In addition to the  $T_g$ , the coefficient of thermal expansion is another thermal property related to the thermal stability of epoxy polymer. The CTE of epoxy nanocomposites containing different formats of graphene were also computed from MD simulation. The simulation procedure is basically the same as that in the calculation of  $T_g$ . When the volume variation corresponding to the temperature change was determined from the MD simulation, the CTE was then calculated as follows:

$$\alpha = \frac{1}{V_0} \frac{\Delta V}{\Delta T} \quad (4)$$

where  $\Delta V$  denotes the volume change associated with the temperature variation of  $\Delta T$ , and the  $V_0$  is the volume of the simulation cell prior to the temperature variation. Note that the range of temperature variation in the calculation of CTE was designated from  $T_g$  to room temperature. The CTE values for the nanocomposites in terms of different formats of graphene are also shown in Table 1. It can be seen that the CTE drops as the graphene is incorporated in the epoxy polymer. Moreover, the introduction of graphene oxide leads to a lower CTE value than in the other cases, and can thus provide great thermal stability in the polymer system. The mechanical properties of epoxy listed in Table 1 were calculated based on the COMPASS force field. From the comparison of the simulation results with the experimental data [28,30,31], it is found that both results coincide quite well. This is the reason we selected the COMPASS force field to characterize the nanocomposites associated with epoxy polymer.

#### 4.4. Calculation of interaction energy

In light of the forgoing properties of graphene nanocomposites, it appears that the graphene oxide can produce better moduli and lower CTE than pristine graphene in the nanocomposites. In order to understand the effect of oxide surface modification, the interaction energy between the graphene and epoxy were calculated as [25]:

Table 1  
Thermal and mechanical properties of epoxy and epoxy nanocomposites in terms of three different formats of graphene.

	Epoxy (Exp.)	Epoxy (Simulation)	Nanocomposites		
			Graphene flakes	Intercalated graphene	Intercalated graphene oxide
Young's modulus (GPa)	3.24[28]	3.16	5.48	5.63	6.36
$T_g$ (K)	377[30]	380	390	400	400
CTE ( $10^{-6}/K$ )	366[31]	362	312	290	284

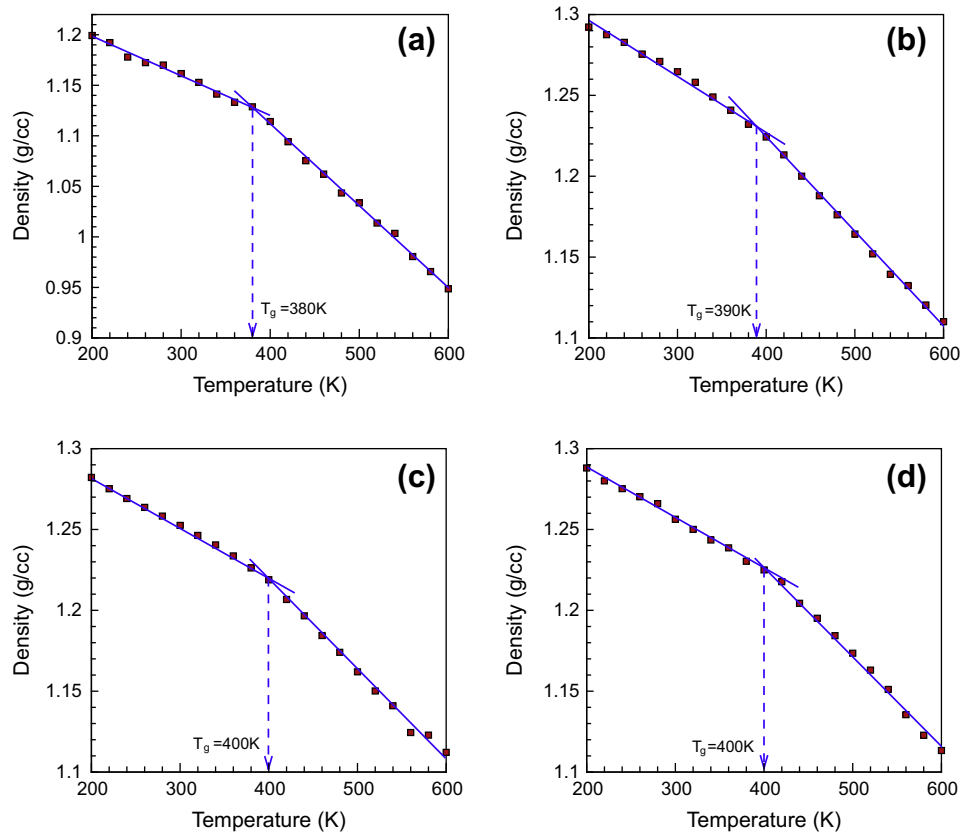


**Fig. 7.** Estimation of glass transition temperature for epoxy and graphene/epoxy nanocomposites ((a) epoxy polymer (b) graphene flakes nanocomposites, (b) intercalated graphene nanocomposites and (c) intercalated graphene oxide nanocomposites).

$$E_{\text{Interaction}} = E_{\text{total}} - E_{\text{graphene}} - E_{\text{epoxy}} \quad (5)$$

where  $E_{\text{total}}$  indicates the total energy of the nanocomposites, as shown in Fig. 8(a). However,  $E_{\text{graphene}}$  and  $E_{\text{epoxy}}$  denote the potential energy of graphene and epoxy, respectively.  $E_{\text{graphene}}$  can be calculated independently from the simulation cell where the polymer was eradicated, as shown in Fig. 8(b). A similar approach was employed to calculate the potential energy of epoxy, as shown in Fig. 8(c). The difference between the total energy of nanocomposites and the potential energy of graphene and epoxy is regarded as the interaction energy between the two constituents. The interaction energy for the graphene with and without surface modification is compared in Table 2. It can be seen the interaction energy in the graphene nanocomposites with surface modification is higher than that of pristine graphene. This higher interaction energy may be responsible for the improved mechanical and thermal properties in graphene oxide nanocomposites.

**Table 2**

Comparison of interaction energy of epoxy associated with graphene and graphene oxide.

	Epoxy/graphene	Epoxy/graphene oxide
Interaction energy (kcal/mol)	−340.25	−460.47

## 5. Conclusions

The mechanical properties of nanocomposites in terms of the three different formats of graphene: intercalated graphene, intercalated graphene oxide and graphene flakes, were explored using MD simulation. Basically, the graphene nanocomposites demonstrate higher moduli, higher glass transition temperature and lower values of CTE than does the pristine polymer without any reinforcements. Moreover, the influences of graphene are more considerable in the nanocomposites with intercalated graphene than are those in the nanocomposites with graphene flakes. By

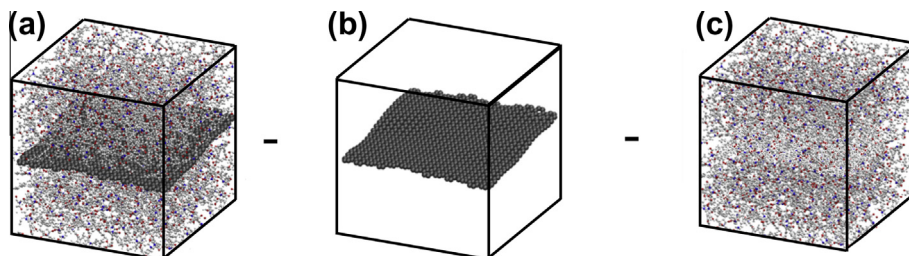


**Fig. 8.** Calculation of interaction energy between graphene and matrix.

observing the morphology of polymer chains, it was found that the local density close to the graphene is relatively high, and there are greater amounts of high density polymers in the intercalated graphene nanocomposites. These high amounts of high density polymer are responsible for the enhanced thermal and mechanical properties in the intercalated nanocomposites. In addition, the graphene oxide can provide a superior reinforcement effect than can the pristine graphene associated with the Young's modulus and CTE of the nanocomposites. The enhanced mechanism was elaborated by the higher interaction energy between the graphene and surrounding matrix in the graphene oxide nanocomposites. In summary, with the combined advantage of the high interaction energy and the high extent of high density polymer, the incorporation of intercalated graphene oxide can lead to the superior thermal and mechanical properties of nanocomposites.

### Acknowledgment

This research was supported by the National Science Council, Taiwan, under the contract no. NSC 99-2212-E-009-023 to National Chiao Tung University.

### References

- [1] Novoselov KS, Geim AK, Morozov SV, Jiang D, Zhang Y, Dubonos SV, et al. Electric field effect in atomically thin carbon films. *Science* 2004;306(5696):666–9.
- [2] Lee C, Wei X, Kysar JW, Hone J. Measurement of the elastic properties and intrinsic strength of monolayer graphene. *Science* 2008;321(5887):385–8.
- [3] Shen XJ, Liu Y, Xiao HM, Feng QP, Yu ZZ, Fu SY. The reinforcing effect of graphene nanosheets on the cryogenic mechanical properties of epoxy resins. *Compos Sci Technol* 2012;72(13):1561–7.
- [4] Lee JK, Song S, Kim B. Functionalized graphene sheets-epoxy based nanocomposite for cryotank composite application. *Polym Compos* 2012;33(8):1263–73.
- [5] Wang S, Tambraparni M, Qiu J, Tipton J, Dean D. Thermal expansion of graphene composites. *Macromolecules* 2009;42(14):5251–5.
- [6] Martín-Gallego M, Verdejo R, Lopez-Manchado MA, Sangermano M. Epoxy-graphene UV-cured nanocomposites. *Polymer* 2011;52(21):4664–9.
- [7] Martín-Gallego M, Hernandez M, Lorenzo V, Verdejo R, Lopez-Manchado MA, Sangermano M. Cationic photocured epoxy nanocomposites filled with different carbon fillers. *Polymer* 2012;53(9):1831–8.
- [8] Tang LC, Wan YJ, Yan D, Pei YB, Zhao L, Li YB, et al. The effect of graphene dispersion on the mechanical properties of graphene/epoxy composites. *Carbon* 2013;60:16–27.
- [9] Rafiee MA, Rafiee J, Wang Z, Song H, Yu ZZ, Koratkar N. Enhanced mechanical properties of nanocomposites at low graphene content. *ACS Nano* 2009;3(12):3884–90.
- [10] Steurer P, Wissert R, Thomann R, Mülhaupt R. Functionalized graphenes and thermoplastic nanocomposites based upon expanded graphite oxide. *Macromol Rapid Commun* 2009;30(4–5):316–27.
- [11] Fang M, Wang K, Lu H, Yang Y, Nutt S. Covalent polymer functionalization of graphene nanosheets and mechanical properties of composites. *J Mater Chem* 2009;19(38):7098–105.
- [12] Ansari S, Giannelis EP. Functionalized graphene sheet-poly(vinylidene fluoride) conductive nanocomposites. *J Polym Sci Pol Phys* 2009;47(9):888–97.
- [13] Ramanathan T, Abdala AA, Stankovich S, Dikin DA, Herrera-Alonso M, Piner RD, et al. Functionalized graphene sheets for polymer nanocomposites. *Nat Nanotechnol* 2008;3(6):327–31.
- [14] Liang J, Huang Y, Zhang L, Wang Y, Ma Y, Guo T, et al. Molecular level dispersion of graphene into poly(vinyl alcohol) and effective reinforcement of their nanocomposites. *Adv Funct Mater* 2009;19(14):2297–302.
- [15] Kim H, Macosko CW. Morphology and properties of polyester/exfoliated graphite nanocomposites. *Macromolecules* 2008;41(9):3317–27.
- [16] Kim H, Macosko CW. Processing-property relationships of polycarbonate/graphene composites. *Polymer* 2009;50(15):3797–809.
- [17] Yadav SK, Cho JW. Functionalized graphene nanoplatelets for enhanced mechanical and thermal properties of polyurethane nanocomposites. *Appl Surf Sci* 2013;266:360–7.
- [18] Zhang LB, Wang JQ, Wang HG, Xu Y, Wang ZF, Li ZP, et al. Preparation, mechanical and thermal properties of functionalized graphene/polyimide nanocomposites. *Composites Part A* 2012;43(9):1537–45.
- [19] An JE, Jeon GW, Jeong YG. Preparation and properties of polypropylene nanocomposites reinforced with exfoliated graphene. *Fibers Polym* 2012;13(4):507–14.
- [20] Bora C, Gogoi P, Baglari S, Dolui SK. Preparation of polyester resin/graphene oxide nanocomposite with improved mechanical strength. *J Appl Polym Sci* 2013;129(6):3432–8.
- [21] Kula T, Khanra P, Mishra AK, Kim NH, Lee JH. Functionalized-graphene/ethylene vinyl acetate co-polymer composites for improved mechanical and thermal properties. *Polym Test* 2012;31(2):282–9.
- [22] Yu S, Yang S, Cho M. Multi-scale modeling of cross-linked epoxy nanocomposites. *Polymer* 2009;50(3):945–52.
- [23] Schniepp HC, Li JL, McAllister MJ, Sai H, Herrera-Alonso M, Adamson DH, et al. Functionalized single graphene sheets derived from splitting graphite oxide. *J Phys Chem B* 2006;110(17):8535–9.
- [24] Szabó T, Berkesi O, Forgó P, Josepovits K, Sanakis Y, Petridis D, et al. Evolution of surface functional groups in a series of progressively oxidized graphite oxides. *Chem Mater* 2006;18(11):2740–9.
- [25] Lv C, Xue Q, Xia D, Ma M, Xie J, Chen H. Effect of chemisorption on the interfacial bonding characteristics of graphene-polymer composites. *J Phys Chem C* 2010;114(14):6588–94.
- [26] Sun H, Ren P, Fried JR. The COMPASS force field: parameterization and validation for phosphazenes. *Comput Theor Polym S* 1998;8(1–2):229–46.
- [27] Materials Studio. User's Manual, Version 1.2. Accelrys, Inc. (San Diego, CA); 2001.
- [28] Zunjarrao SC, Singh RP. Characterization of the fracture behavior of epoxy reinforced with nanometer and micrometer sized aluminum particles. *Compos Sci Technol* 2006;66(13):2296–305.
- [29] Theodorou DN, Suter UW. Atomistic modeling of mechanical properties of polymeric glasses. *Macromolecules* 1986;19(1):139–54.
- [30] Mukherjee N, Wavhal D, Timmons RB. Composites of plasma surface functionalized barium titanate nanoparticles covalently attached to epoxide matrices: synthesis and evaluation. *ACS Appl Mater Int* 2010;2(2):397–407.
- [31] He Y, Li Q, Kula T, Kim NH, Jiang TW, Lau K, et al. Micro crack behavior of carbon fiber reinforced thermoplastic modified epoxy composites for cryogenic applications. *Composites Part B* 2012;44(1):533–9.